Revealing the Nature of Trapping Sites in Nanocrystalline Titanium Dioxide by Selective Surface Modification†

Nada M. Dimitrijevic,* Zoran V. Saponjic, David M. Bartels, Marion C. Thurnauer, David M. Tiede, and Tijana Rajh*

Chemistry Division, Argonne National Laboratory, Argonne, Illinois 60439

Received: January 10, 2003; In Final Form: April 3, 2003

Excess electrons in nanocrystalline TiO_2 were studied in bare and dopamine-capped TiO_2 nanoparticles by electron-beam pulse radiolysis. Reaction of hydrated electrons with dopamine-capped TiO_2 nanoparticles was found to be at the diffusion-controlled limit, $k = 1 \times 10^{11}$ M^{-1} s^{-1}, while the reaction with 1-hydroxy-1-methylethyl radicals, $(CH_3)_2\dot{C}OH$, was 2 orders of magnitude slower, $k = 4 \times 10^8$ M^{-1} s^{-1}. The reactions result in injection of electrons into the conduction band of TiO_2 nanoparticles. Optical absorption spectra of injected excess electrons in dopamine-capped nanoparticles display monotonic featureless wavelength dependence up to 1800 nm. In contrast, bare particles have shown two preferential optical transitions with energies in the visible region ($\lambda_{max} = 670$ nm and $\lambda_{max} = 900$ nm). Flat band potential of dopamine-capped TiO_2 nanoparticles was shifted by 100 mV to more negative values. The strong coupling of dopamine to surface Ti atoms was also found to improve the separation of photogenerated charges. This was demonstrated by the enhanced efficiency of photogenerated electrons in reducing silver cations to metallic silver in systems linked via a dopamine bridge, compared to the same systems linked through carboxyl groups.

Introduction

Control of surface chemistry, particle shape, and particle organization of nanocrystalline materials has gained considerable attention primarily because of their unique chemistry (enhanced chemical reactivity, specific syntheses, enhanced catalytic activity, hardening of materials, specific bindings, etc.). Titanium dioxide is the photocatalytic material that has been studied most extensively over the past 10 years because it is an inexpensive, nontoxic, and photostable material.[1] Nanoparticulate TiO_2 has been studied as a light-harvesting material for potential use in photocatalytic removal of hazardous industrial byproducts[2−4] or in nanocrystalline solar cells.[5−9] The mechanism of semiconductor-assisted photocatalysis is based on the principle that particulate semiconductors behave as miniature photoelectrochemical cells. Although TiO_2 is very effective from an energetic point of view, it is a relatively inefficient photocatalyst. The main energy loss is due to the recombination of charges generated upon excitation of TiO_2, which is manifested as the relatively low efficiency of long-lived charge separation. In addition, because of its large band gap ($E_g = 3.2$ eV), TiO_2 absorbs less than 5% of the available solar light photons. Hence, the main research interests concerning application of nanocrystalline TiO_2 are focused on improvement of the separation of charges, as well as the efficiency for visible light absorption. Two approaches, based on surface modification of TiO_2 with dye molecules or multifunctional ligands, have been pursued. Dye sensitization of wide band gap semiconductors via photoinduced interfacial electron transfer from excited dyes[5−9] has been a topic of continuing interest because of the extension of the semiconductor response into the solar spectrum due to the dye absorption. The second approach involves adjusting the electronic properties of nanocrystalline particles by adsorption of electron-donating bidentate enediol ligands.[10−13] This results in instantaneous long-range charge separation between organic ligands covalently linked to the surface atoms and the conduction band of semiconductor nanoparticles. This approach also extends semiconductor response into the solar spectrum due to the electronic coupling of π states of ligands with the conduction band states of semiconductor nanoparticles.

Enhanced coupling of multifunctional ligands results also in passivation of the surface states.[13] X-ray absorption spectroscopic (XAS) studies have shown that the surface states in TiO_2 nanocrystallites are actually coordinately unsaturated Ti sites that are formed upon surface reconstruction of nanoparticles.[14] Electron paramagnetic resonance (EPR) studies have shown that the majority of photogenerated electrons are trapped on these undercoordinated surface sites.[13,15] However, when the surface Ti atoms in nanoparticles are coupled with enediol ligands, XAS studies indicate restructuring of the undercoordinated surface sites into their optimal octahedral structure. Concomitantly, EPR spectra indicate removal of the surface undercoordinated sites. Illumination of nanoparticles surface-modified with enediol ligands resulted in the appearance of two very strong and narrow axially symmetric EPR signals in the $g < 2$ region [Ti(III) character] well resolved in the parallel orientation characteristic of electrons in an anatase lattice environment.

In this paper we describe the study of the effect of enediol modification of surface Ti atoms on the electronic properties of excess electrons injected by electron-beam radiolysis. We have used an electron pulse radiolysis technique to selectively inject electrons in dopamine-capped TiO_2 and study their optical properties. This technique enables examination of excess electrons without interference of positive holes present in photoexcitation experiments. Comparison of the optical absorption spectra in bare and capped TiO_2 leads to understanding of the nature of surface trapping sites and reports on the ability of enediol ligands to repair the coordination of surface Ti atoms to a bulklike structure isoenergetic with the conduction band

† Part of the special issue "Arnim Henglein Festschrift".

10.1021/jp034064i CCC: $25.00
Published on Web 06/04/2003

of TiO_2 nanoparticles. Additionally, ligation of the surface Ti atoms with the enediol ligands can change reduction properties of charge carriers in small-particle TiO_2. We have determined the flat band potential of the dopamine-capped TiO_2 in order to address the reducing power of these particles. The effect of strong coupling of dopamine modifier on the efficiency of charge separation was monitored by the deposition of metallic silver.

Experimental Section

All chemicals used were of highest commercial purity and were used without further purification. ASTM type I water or D_2O (for transient absorption in near-IR) was used. The preparation and characterization of dopamine-modified TiO_2 is described elsewhere[13] and only outlined here. The seeds of colloidal TiO_2 were prepared by dropwise addition of titanium(IV) chloride to cooled water with an apparatus developed for controlling temperature and rate of mixing reaction components.[11,15] Slow growth of the particles was achieved by dialysis at 4 °C against water until the pH of the solution reached 3.5, when the growth of crystalline particle TiO_2 was complete. Capping of TiO_2 particles by surface modification that resulted in the formation of a charge-transfer complex was achieved by addition of surface-active ligands at concentrations required to cover all surface sites. The dopamine-capped TiO_2 colloids (TiO_2/DA), onset of absorption $\lambda \approx 760$ nm, were then dialyzed against H_2O or D_2O, pH 3.5. The pH was adjusted with $HClO_4$. The titania particles were 42.8 ± 3.5 Å in diameter. Additionally, TiO_2 particles with partial dopamine coverage of surface Ti centers were prepared by the addition of appropriate amounts of dopamine into TiO_2 colloidal suspensions prepared in D_2O.

The modification of TiO_2 particles with carboxyethyl-β-cyclodextrin, CE-β-CD, was obtained by mixing solutions of the two components in desired proportions. The conjugation of CE-β-CD onto TiO_2/DA particles via carboxyl groups on cyclodextrin and amino groups on dopamine was performed by a condensation reaction[16] via the intermediate *N*-hydroxysuccinimide ester modified and optimized for linking to TiO_2 nanoparticles. Typically, 20 mg of *O*-(*N*-succinimidyl)-*N*,*N*,*N*,*N*-tetramethyluroniumtetrafluoroborate (TSU) and 30 μL of *N*,*N*-diiodopropylethylamine were consecutively added into 2 mL of 0.1 mM CE-β-CD. The solution was dialyzed against water (molecular weight cutoff 500) in order to remove unreacted TSU. After dialysis, 0.4 mg of dopamine was added, and the solution was incubated for 24 h in the dark. After incubation, 0.2 mL of solution was added to 1 mL of 10 mM TiO_2 (molar concentration). The solution of TiO_2/DA/CE-β-CD was dialyzed against water, pH 3.5 (3500 MW cutoff), in order to remove nonbound CE-β-CD. All dialysis steps were performed under nitrogen atmosphere. The coverage of the surface by dopamine was 5.7%, and each TiO_2 particle was linked to approximately two molecules of CE-β-CD.

Apparatus. Electron pulse radiolysis experiments were performed at the Argonne 20 MeV linear accelerator. Two different pulse radiolysis setups were used, one for the short-time resolution (up to 100 μs) and another for longer times (from 1 ms to 10 s). In both cases transient species were detected optically.

For short-time experiments, photomultiplier (Hamamatsu R-1913), interference filters (bandwidth 50 nm), and silicon or InGaAs photodiodes (EG&G FND100 and germanium power device GAP520, respectively) were used as optical detectors. The silicon photodiode was used for measurements of the rate constant of hydrated electrons with TiO_2/DA particles in H_2O solution at 650 nm. The InGaAs photodiode was used for measurements of the spectra of excess electrons in nanoparticles in D_2O solutions in the wavelength region up to 1800 nm. The electron pulses were collinear with the analyzing light beam but in the opposite direction.

A commercial Olis RSM 1000 rapid-scanning monochromator system was used for long-time experiments. It consists of a subtractive double monochromator ($^1/_4$ m, f/4.4) with a rotating sector slit at the intermediate focal plane to scan the wavelength, a beam splitter, a pair of photomultipliers, and 14-bit 1 MHz digitizers to acquire I_t and I_0 signals. A 250-nm-wide spectrum is acquired every millisecond. For these experiments, electrons entered the cell perpendicular to the analyzing light. Details are given elsewhere.[17]

The dose in the cell was measured by use of aerated solutions of thiocyanate and hexacyanoferrate(II).[18,19] For dosimetry in long-time experiments the "super Fricke" solution was used.[18] The absorbed dose in a sample was varied by changing the duration of electron pulses and ranged from 21 to 288 Gy/pulse. All measurements were done at room temperature.

For the experiments in heavy water, deuterated *tert*-butyl alcohol, $(CD_3)_3COD$, was used as a scavenger of OD and D radicals.

FTIR spectra were measured on a Nicolet 510 Fourier transform infrared spectrophotometer equipped with a Spectra Tech diffuse reflectance accessory. Samples were collected as dry material and measured as 8 wt % in KBr matrix. Typically 100 scans were performed for each spectrum. The resolution was 4 cm^{-1}. Results are presented as Kubelka−Munk plots. Samples were illuminated with a Xe 300-W lamp (ILC).

Specimens for observation in the transmission electron microscope (TEM) were prepared by placing 1 or 2 drops of colloidal solution onto holey carbon films supported on copper grids. These specimens were allowed to air-dry for at least 12 h. Specimens were imaged in a Jeol 100CXII TEM operating at 100 kV. High-resolution TEM measurements were carried out on a Jeol 4000EXII TEM operating at 400 kV to record lattice images of individual particles.

Results and Discussion

Excitation of nanocrystalline TiO_2 with photon energies larger than its band gap results in formation of conduction band electrons and valence band holes. Localization of conduction band electrons into lower energy electronic sites occurs in less than 30 ps.[20−23] Due to the large number of electron surface trapping states in nanocrystalline particles, electrons localize preferentially at the TiO_2 surface.[13,24,25] Surface-trapped electrons exhibit broad absorption in the visible region of the spectrum with a maximum around 620 nm in acidic solution.[26−29] The position of absorption maximum varies some 50 nm with the size of the particles and the number of excess electrons.[29] On the other hand, the absorption of electrons in larger particles increases steadily from 400 nm toward longer wavelengths, having a plateau near 900 nm. This absorption feature was attributed to delocalized electrons.[25,28,29]

To probe the nature of surface trapping sites and their selective removal upon binding of surface-active species, we studied and compared optical absorption spectra of excess electrons in bare TiO_2 and dopamine-capped TiO_2 (TiO_2/DA) nanoparticles using an electron pulse radiolysis technique. Our approach is to investigate the electronic structure of trapping sites by controlled injection of excess electrons into empty electron states of nanoparticles while selectively blocking the surface trapping sites by surface modification with bidentate

ligands. The electron pulse radiolysis of aqueous solutions enables selective formation of reducing radicals and, as a time-resolved technique, allows observation of the dynamics of charge-transfer reactions between reducing radicals and nanoparticles. Reducing radicals formed during radiolysis have, in general, high reducing potentials and transfer electrons to the nanoparticles, thereby raising the equilibrium chemical potential of the whole system. As a result, excess electrons are stable and do not decay unless electron acceptors (such as molecular oxygen) are released into the system. Consequently, electron pulse radiolysis enables determination of electronic structure and redox properties of dispersed nanoparticles.

The principle behind electron-beam radiolysis of aqueous solutions is that highly energetic electrons lose their excess energy in collision with water molecules, forming highly energetic radicals (e_{aq}^-, H, OH), and molecular (H_2O_2, H_2) species homogeneously distributed throughout the irradiated sample. The reducing radical species, hydrated electrons and H atoms, have a large negative potential for electron donation, $E°(e_{aq}^-) = -2.77$ V (vs NHE)[30] and $E°(H) = -2.31$ V (vs NHE),[31] respectively, and are capable of injecting electrons into the conduction band of TiO_2/DA particles. Oxidizing OH radicals can be efficiently scavenged by alcohols such as 2-propanol, *tert*-butyl alcohol, etc.

Excess Electrons in Dopamine-Capped TiO_2 Particles. TiO_2 is a semiconductor that has particularly reactive photogenerated positive holes ($E°_{VB} = 2.93$ V vs NHE at pH 3.5) and moderately reactive photogenerated electrons ($E°_{CB} = -0.27$ V vs NHE at pH 3.5).[32] When the metal oxide particles are in the nanocrystalline regime, a large fraction of the atoms that constitute the nanoparticle are located at the surface with significantly altered electrochemical properties. Due to the truncation of the crystal units at the surface and their weaker covalent bonding with solvent species compared to the bonding within the lattice, the energy level of the surface species are found in the mid-gap region, thereby decreasing their reducing/oxidizing abilities.[33] In this paper we investigate optical properties of electrons injected into these mid-gap empty electronic states in TiO_2 nanoparticles from radiolytically generated reducing radical species e_{aq}^- and H atoms. Also, electrons were injected into TiO_2 nanoparticles capped with enediol ligands such as dopamine that were shown to remove surface trapping sites in nanocrystalline TiO_2. We have investigated capped TiO_2/DA particles that were 4.3 nm in diameter, with dopamine covering 90% of the existing 405 titanium surface sites/particle (maximum coverage).[13]

Pulse radiolysis experiments were carried out in nitrogen-saturated aqueous solution of colloidal particles at pH 3.5 and in the presence of a high concentration of *tert*-BuOH (2 M), in which the following reactions occur:

$$OH/H + (CH_3)_3COH \rightarrow H_2O/H_2 + C_4H_8OH \quad (1)$$

$$e_{aq}^- + TiO_2/DA \rightarrow (e^-)TiO_2/DA \quad (2)$$

$$e_{aq}^- + H^+ \rightarrow H \quad (3)$$

$$H + TiO_2/DA \rightarrow (e^-)TiO_2/DA + H^+ \quad (4)$$

The oxidizing radical species OH reacts with *tert*-BuOH, which is an efficient scavenger of OH ($k_1 = 4 \times 10^8$ M^{-1} s^{-1}) and to a lesser extent of H radicals ($k_1 = 10^5$ M^{-1} s^{-1}); the product of reaction 1 is inert toward TiO_2 and/or dopamine.[34,35] The concentration of TiO_2/DA in solution was kept high (0.16 mM particle concentration) in order to overcome possible competition between the reactions of nanoparticles and H^+ ions with hydrated electrons ($k_3 = 2.0 \times 10^{10}$ M^{-1} s^{-1}). In this case, the concentration of free dopamine in solution was $\leq$0.1 mM, determined from the association constant of the dopamine with titania particles, $K = 7.9 \times 10^3$ M^{-1}.[13] Under these conditions, approximately half of the generated H atoms will not be scavenged with *tert*-BuOH. Remaining hydrogen atoms will participate directly in reducing TiO_2/DA particles, based on the rate constant for the reaction of H atoms with bare TiO_2 particles, $k = 2 \times 10^9$ M^{-1} s^{-1},[34] or they can react with free dopamine (DA):

$$H + DA \rightarrow DA^- + H^+, \; k = 4.2 \times 10^9 \text{ M}^{-1} \text{ s}^{-1}\,[35] \quad (5)$$

Reduced dopamine radicals, DA^-, have a sufficiently large negative redox potential of -1.9 V vs NHE[35] to be able to transfer electrons into TiO_2/DA particles:

$$DA^- + TiO_2/DA \rightarrow (e^-)TiO_2/DA + DA \quad (6)$$

Dopamine radical anions exhibit absorption below 400 nm and, thus, do not interfere with our measurements at wavelengths longer than 600 nm.

Whatever the fate of H atoms that are not scavenged with *tert*-BuOH, *the net effect is generation of excess electrons into the particles* (reactions 2−6). However, because the yield of H atoms is at least 5 times lower than that of e_{aq}^-, the majority of electrons injected into TiO_2/DA particles come from reaction 2. Free dopamine does not compete with either H^+ ions or nanoparticles for hydrated electrons because of the very low rate of any possible reaction, $\leq 2 \times 10^4$ s^{-1}.[35]

The absorption of excess electrons in 43 Å anatase nanoparticles was measured in the range 600−1800 nm, after the decay of hydrated electron absorption. A typical transient absorption signal of hydrated electrons at 650 nm is presented in Figure 1a. In the absence of nanoparticles, the decay of absorption is due to the reaction of hydrated electrons with hydronium ions, reaction 3. When TiO_2 or TiO_2/DA particles are present in the solution, the fast decay of transient absorption corresponds to the reaction of e_{aq}^- with particles. The excess electrons in particles exhibit long-lived transient absorption (see Figure 1b) throughout the whole range of examined wavelengths.

Transient absorption spectra measured at 0.8 μs after the pulse in N_2-saturated heavy water solution of 0.16 mM nanoparticles and 2 M *tert*-BuOH-d_{10} are presented in Figure 2. The dose was kept low, 152.2 Gy/pulse, to produce less than 1 electron/particle. The spectrum of excess electrons in bare TiO_2 shows a broad band with a maximum around 670 nm and flat absorption in the range 1200−1800 nm. The appearance of a broad band in the absorption spectrum correlates to the spectra of trapped electrons in TiO_2 observed previously in the range 400−1200 nm.[26−29] It was found that these surface trapping sites in nanosize TiO_2 particles experience an adjustment in the coordination geometry of the Ti atoms near the particle surface from octahedral to square-pyramidal in order to accommodate for large surface curvature.[13] The coordination sphere of the surface titanium atoms is incomplete and thus exhibits high affinity for oxygen-containing ligands to form chelating structures. X-ray absorption near edge structure (XANES) reveals that surface modification with enediol ligands such as dopamine restores the pre-edge features of octahedrally coordinated Ti in the anatase crystal environment and removes surface trapping sites.

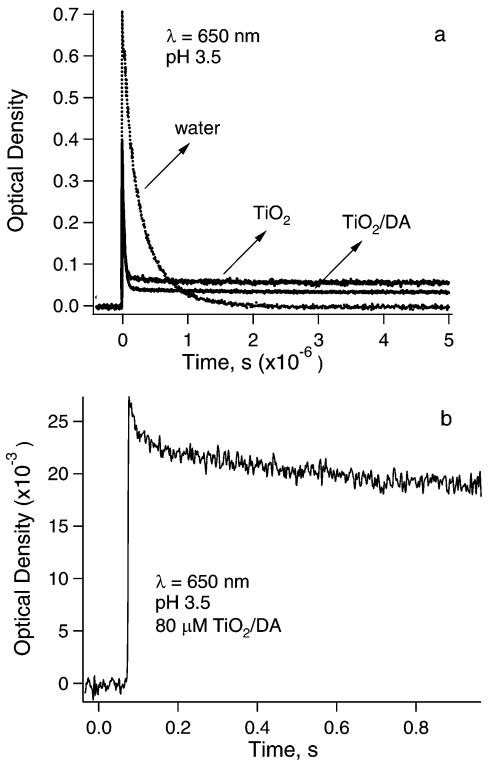

Figure 1. (a) Transient absorption signals at 650 nm measured in N_2-saturated solution of 2 M *tert*-BuOH, pH 3.5, in the absence of particles (water) and in the presence of 43 Å TiO_2 or TiO_2/DA particles. Particle concentration is 160 μM. Dose was 138.0 Gy/pulse. (b) Transient absorption signal at 650 nm of 80 μM TiO_2/DA and 2 M *tert*-BuOH recorded up to 1 s. Dose was 123.8 Gy/pulse.

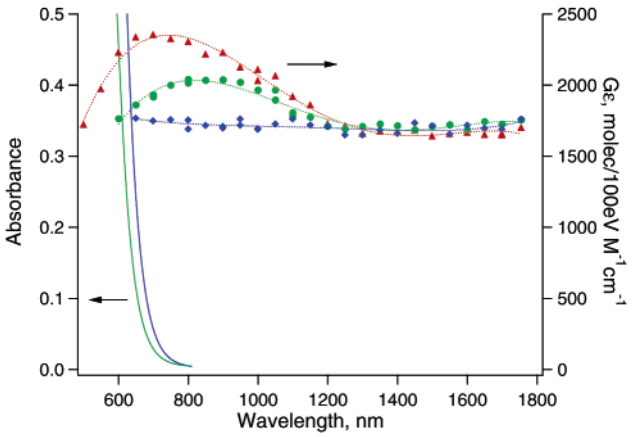

Figure 2. Transient absorption spectra observed 0.8 μs after pulse in N_2-saturated D_2O solution of 2 M *tert*-BuOH-d_{10} and 160 μM (▲) bare TiO_2, and (◆) capped TiO_2/DA particles, pH 3.5. The spectrum presented with circles (●) is obtained for TiO_2 particles with only 70% of surface sites covered with dopamine. Dose was 152.2 Gy/pulse. The figure contains absorption spectra of dopamine-modified TiO_2 particles with 70% (green line) and full coverage (blue line) of the surface states.

When the surface of the nanoparticles is partially covered with dopamine (surface coverage of only 70%), the maximum absorption at 670 nm observed for excess electrons in bare TiO_2 disappears and a new maximum corresponding to excess electrons at 900 nm appears, while the flat region of the spectrum in the range 1200−1800 nm remains unchanged (Figure 2, ●). The lower yield of absorption that corresponds to trapped electrons, as well as the shift of absorption maximum toward lower energies, indicates that the deepest surface sites are repaired primarily and that the electrons localize at the remaining surface centers. This spectrum is identical to the spectrum of excess electrons in large particles or aged anatase colloids, reported previously and assigned to the conduction band electrons.[25,28,29]

When the surface of particles is completely covered with a monolayer of dopamine (TiO_2/DA particles) that converts undercoordinated Ti sites into anatase-like octahedral Ti surface atoms, the spectrum of excess electrons in titania becomes featureless, appearing as a monotonic absorption in the whole range from 600 to 1800 nm. This spectrum is characteristic for electrons that are not localized on surface trapping sites whose energy of localization is ≤0.7 eV below the conduction band. The dependence of the absorption coefficient on the wavelength does not show a characteristic exponential Drude behavior (λ^2)[36] expected for free carrier absorption. This result suggests that the overall spectrum is a consequence of either (i) superposition of the multiple absorption features created from broad distribution of energies of shallow trapping states in disordered particles or (ii) superposition of free carriers and intersubband absorptions in indirect semiconductors. In the first case the particle disorder would reflect on the EPR spectra, causing broadening of the signals of excess electrons. Our EPR measurements do not support this mechanism because vary narrow signals (ΔH_{pp} = 2.5 G)[10,13] of photogenerated electrons were observed. However, contribution of long-range disorder to overall absorption spectra cannot be excluded.[37] In the second case, contribution of intersubband transitions to overall absorption spectrum in indirect semiconductors[36] results in the flat monotonic absorption in the region 0.6−2.0 eV, assuming energy difference 1.0 eV < ΔE < 1.5 eV between the two lowest subbands of anatase conduction band. XANES measurements in nanoparticulate TiO_2,[10,12] as well as multiple scattering calculations of XAS in bulk anatase TiO_2,[38] report the energy difference of subbands as ∼1.4 eV. In this case the dominant contribution of free carrier absorption is expected at wavelengths further into the IR ($\lambda \geq$ 2.5 μm). Our future research in mid- and far-IR regions will address these issues.

The disappearance of the maximum absorption confirms that surface trapping sites have been repaired by the bidentate DA ligands. The ability of DA to replace surface five-coordinated Ti (defect sites) into octahedral surface Ti states promotes formation of the bulklike surface, making nanocrystallites into bulklike material. From our results we can conclude that modification of TiO_2 with dopamine suppresses/repairs defect sites that are deeper than ∼0.6 eV below the conduction band. The absorption spectra reported here are also in agreement with EPR measurements of the photogenerated electrons in TiO_2 particles modified with enediol ligands.[13] The EPR spectra of electrons in dopamine-modified TiO_2 have shown delocalized sites, in addition to localized lattice-Ti^{3+} centers. As mentioned above, measurements in mid- and far-IR are needed for full understanding of the ability of enediol ligands to suppress trapping sites reported earlier to be 0.42−0.5 eV below the conduction band.[25,39]

In Figure 3a, optical signals at 1000 and 1700 nm for a solution containing TiO_2/DA particles are presented. The 1000 nm signal corresponds to the decay of hydrated electrons in D_2O, while the signal at 1700 nm corresponds to the formation of lattice electrons in well-crystallized TiO_2 particles covered with dopamine (Figure 3b). The rates of decay and formation agree within 20%. The signals were not corrected for the delayed secondary response of the InGaAs photodiode.[40] For these particular two wavelengths, the distortion of optical signals is almost identical and small, amounting to 10% of the true optical

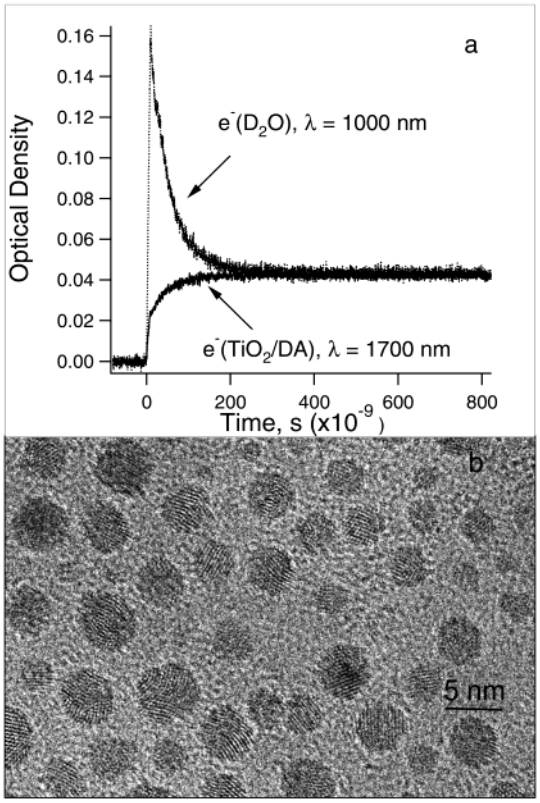

Figure 3. (a) Transient absorption signals detected at 1000 and 1700 nm after 152.2 Gy electron pulse in N_2-saturated D_2O solution of 2 M *tert*-BuOH-d_{10} and 160 μM TiO_2/DA particles. (b) High-resolution TEM images of TiO_2 particles.

signal.[40] The agreement between rates of decay and formation confirms that injection of excess electrons into capped TiO_2/DA particles proceeds predominantly through reaction with hydrated electrons.

Reaction Rates. The rate constant for the reaction of hydrated electrons with TiO_2/DA, reaction 2, was determined by changing the concentration of particles and measuring the decay of hydrated electron absorption at 650 nm. The particle concentration was determined from the average particle diameter 42.8 ± 3.5 Å and total concentration of TiO_2. Figure 4 presents transient absorption signals detected after a pulse of electrons in a pH 3.5 aqueous solution containing 2 M *tert*-BuOH and various concentrations of TiO_2/DA. The bimolecular rate constant, $k_1 = (1.0 \pm 0.3) \times 10^{11}$ M^{-1} s^{-1}, was determined from the slope of the linear plot of pseudo-first-order rates (Figure 4, inset). We have found that the reaction of hydrated electrons with TiO_2/DA particles is 2 times slower than the corresponding reaction with bare TiO_2. The value of 2.1×10^{11} M^{-1} s^{-1} was estimated from the decay of e_{aq}^- absorption in the presence of 0.16 mM TiO_2 particles. At pH 3.5, dopamine is a charged molecule (pK = 8.9);[35] therefore, it can alter the surface charge of modified TiO_2 particles and alter the reaction rate of particles with negatively charged solvated electrons. This value is approximately 2 times smaller than the one reported previously[34] for highly charged 4.7 nm bare TiO_2 particles at pH 2.65, derived from competition kinetics. On the other hand, these values of the rate constant for bare TiO_2 in acidic solution are 2 orders of magnitude larger than the one at pH 10, when the surface of TiO_2 is negatively charged.[41]

The rate constant for the reaction of 1-hydroxy-1-methylethyl radicals, $(CH_3)_2\dot{C}OH$, with TiO_2/DA was estimated from the growth of the absorption after the pulse in N_2-saturated solution

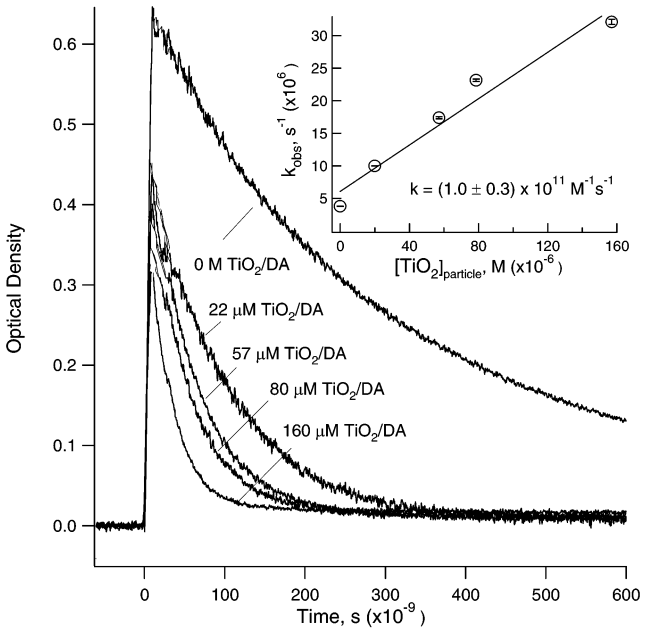

Figure 4. Absorption−time profiles (650 nm) of hydrated electrons at different particle concentrations of capped TiO_2/DA. Dose was 138.0 Gy/pulse. Inset shows the dependence of the observed decay rates as a function of particle concentration.

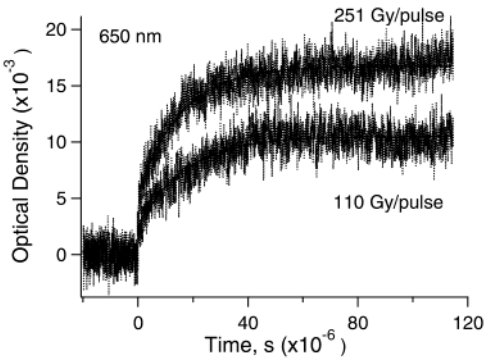

Figure 5. Growth of absorption at 650 nm after the 251 and 110 Gy electron pulses in N_2-saturated solution of 2 M acetone, 1 M 2-PrOH, and 0.1 mM TiO_2/DA particles, pH 3.5.

containing 2 M acetone, 1 M 2-propanol, and 0.1 mM TiO_2/DA particles. In this system the following reactions occur:

$$e_{aq}^- + (CH_3)_2CO + H_2O \rightarrow (CH_3)_2\dot{C}OH + OH^- \quad (7)$$

$$OH/H + (CH_3)_2CHOH \rightarrow H_2O/H_2 + (CH_3)_2\dot{C}OH \quad (8)$$

$$2(CH_3)_2\dot{C}OH \rightarrow (CH_3)_2CHOH + (CH_3)_2CO \quad (9)$$

$$(CH_3)_2\dot{C}OH + TiO_2/DA \rightarrow (e^-)TiO_2/DA + (CH_3)_2CO + H^+ \quad (10)$$

The $(CH_3)_2\dot{C}OH$ radicals, $E^\circ[(CH_3)_2\dot{C}OH] = -1.8$ V (vs NHE),[42] formed in reactions 7 and 8 inject electrons into capped TiO_2/DA particles. The bimolecular rate constant for the reaction of $(CH_3)_2\dot{C}OH$ radicals with TiO_2/DA particles, $k_{10} = 4 \times 10^8$ M^{-1} s^{-1}, was determined from the growth of the transient absorption at 650 nm that corresponds to the injected excess electrons in particles (Figure 5). The value agrees with the data reported for 4.7 nm bare TiO_2 particles.[34]

The electron-transfer reaction on the surface of semiconductor particles is a heterogeneous process that involves the movement

of reducing radicals through the Helmholtz double layer. The rate constant for the interfacial electron transfer from reducing radicals into TiO_2 particles, k_{et} (centimeters per second), is related to the observed bimolecular rate constants of the electron-transfer reactions, k_{obs} (liters per mole per second):[43,44]

$$\frac{1}{k_{obs}} = \frac{1000}{4\pi r_r^2 N_A}\left(\frac{1}{k_{et}} + \frac{r_r}{D}\right) \tag{11}$$

where r_r (centimeters) is the reaction radius corresponding to the sum of the radii of particles and radicals, D (square centimeters per second) is the sum of their respective diffusion constants, and N_A is Avogadro's number. For $k_{et} \ll D/r_r$, the interfacial electron transfer is a rate-limiting process, and k_{et} can be calculated from

$$k_{et} = \frac{1000 k_{obs}}{4\pi r_r^2 N_A} \tag{12}$$

The values for k_{et} of 2.6×10^2 and 1.0 cm/s were calculated from the above equation for the reaction of TiO_2/DA particles with hydrated electrons and 1-hydroxy-1-methylethyl radicals at pH 3.5, respectively. Equation 12 applies for the uncharged radicals, such as 1-hydroxy-1-methylethyl radicals. On the other hand, the electrical double layer surrounding positively charged colloidal particles affects their reaction with negatively charged hydrated electrons, and the rate constant of interfacial charge-transfer reaction k_{et} then depends on the ζ potential of particles.[45] However, the corrections for the double layer could not change the calculated value of k_{et} of reaction 2 by more than 50%.[45] The 2 orders of magnitude difference in k_{et} observed for e_{aq}^- and $(CH_3)_2\dot{C}OH$ radicals indicate the effect of the driving force as a result of the difference in redox potential of examined radicals.

It has been shown that the rate constant of charge-transfer reaction on the surface of TiO_2 particles, k_{et}, depends on the overall driving force, expressed as a difference between standard redox potential of electron-donating radicals in solution, R, and that of conduction band electrons, $E°(R/R^-) - E_{CB}$:[34,43−47]

$$k_{et} = k_{et}^{\circ} \exp\left[-\frac{\alpha}{0.059}(E°(R/R^-) - E_{CB})\right] \tag{13}$$

where k_{et}° is the value of the interfacial rate constant at $E°(R/R^-) - E_{CB} = 0$ and α is the transfer coefficient. Taking into account the value of flat band potential of −0.36 V (vs NHE) determined experimentally (see below), the values for the overall driving force are −2.41 and −1.44 V for the reaction of e_{aq}^- and $(CH_3)_2\dot{C}OH$ radicals with TiO_2/DA, respectively. The driving force in both cases is large and exceeds the total reorganization energy. For these differences in potentials, the values of k_{et} for TiO_2/DA particles are comparable with the values for bare TiO_2.[34,43−47] This confirms electron-transfer reactions of examined radicals with TiO_2/DA semiconductor particles as a whole, not with an isolated, small molecule dopamine on the surface of particles. For small molecules, the bimolecular rate constants for charge-transfer reactions do not change more than an order of magnitude with these radicals.[48] The reaction of hydrated electrons with TiO_2/DA particles probably approaches the mass-transfer limit. The higher reactivity of hydrated electrons toward the bare as compared to the dopamine-capped TiO_2 particles is a result of the changes in the surface charge of TiO_2 particles upon modification.

Redox Potential of TiO_2/DA Particles. Knowledge of the band edge position of semiconductors is a necessary parameter for determination of thermodynamic limitations of photoinduced chemical reactions; i.e., it determines which chemical reaction can be carried out. Photogenerated carriers migrate to the particle surface and participate in reduction and oxidation processes at the surface. The thermodynamic limit for the reaction that can be carried out with the photogenerated charge carriers is given by the position of the band edges (i.e., flat band potential). For example, if a reduction of a particular species in the solution is desired, the conduction band of the semiconductor must be more negative than the relevant redox level, while for the oxidation of the particular species, valence band holes must have more positive potential than the relevant redox potential. Thus, the relative position of the band edges in a given semiconductor determines their redox functioning.

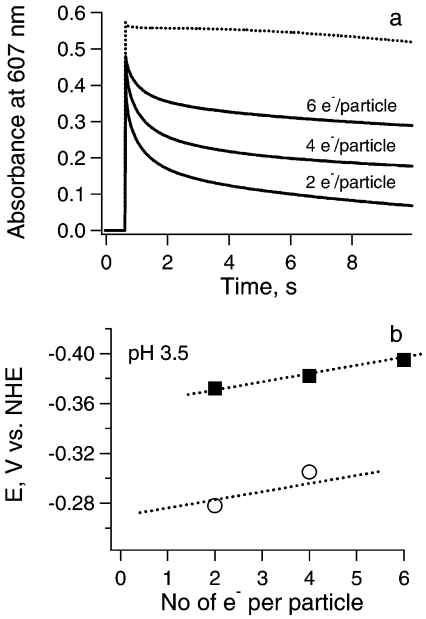

Figure 6. (a) Absorbance at 607 nm after 65.2 Gy repeated pulses in N_2-saturated solution of 0.5 mM MV^{2+} and 1 M 2-PrOH, in the absence (dotted line) and in the presence (solid lines) of 17 μM TiO_2/DA particles, pH 3.5. (b) Changes in the flat band potential with the number of injected excess electrons for (○) bare TiO_2 and (■) capped TiO_2/DA particles. The values for flat band potentials were determined from the equilibrium of reaction 14.

The electron-transfer reaction between methyl viologen, MV^+, and TiO_2/DA was employed for determining the redox potential of particles:

$$n MV^+ + TiO_2/DA \Leftrightarrow (e^-)_n TiO_2/DA + n MV^{2+} \tag{14}$$

where MV^+ is a monovalent cation radical produced as a sole radical species 100 μs after the electron pulse (aqueous solutions containing 2-propanol in nitrogen atmosphere).[49,50] When produced in relatively large concentrations compared to the divalent molecule, MV^+ radicals in solution have a chemical potential more negative than the flat band potential of TiO_2 and inject electrons into nanoparticles. The reaction reaches equilibrium when the redox potential of particles, $E(e^-)$, equilibrates with the redox potential of a couple in the solution:

$$E(e^-) = E°(MV^{2+}/MV^+) + \frac{RT}{zF}\log\frac{MV^{2+}}{MV^+} \tag{15}$$

Figure 6a shows the decay of transient absorption of MV^+ detected at 607 nm in the presence of TiO_2/DA particles. The solutions contained 0.5 mM MV^{2+}, 1 M 2-PrOH, and 17 μM

TiO_2/DA particles. MV^+ was produced in reactions of hydrated electrons and $(CH_3)_2\dot{C}OH$ radicals with MV^{2+}.[49,50] The redox potential of TiO_2/DA particles was calculated from eq 15, taking -0.44 V (vs NHE) for the standard redox potential of the MV^{2+}/MV^+ pair and determining the equilibrium concentration of MV^+ from its known extinction coefficient at absorption maximum, $\epsilon_{607} = 1.37 \times 10^4\ M^{-1}\ cm^{-1}$.[51] Figure 6b shows determined values for both dopamine-capped and bare TiO_2 particles at pH 3.5. The changes in Fermi level position toward more negative values with the number of injected electrons were observed and attributed to the increase in electron density.[36] It was found that the flat band potential of capped TiO_2/DA nanoparticles is 100 mV more negative than the flat band potential of bare TiO_2. We have demonstrated previously[13] that dopamine replaces surface OH groups on TiO_2 and coordinates surface Ti atoms with both OH groups of dopamine, resulting in the overlap of the ligand orbitals with six-coordinated titanium. The enediol complex induces a dipole moment on the surface of particles that alters electronic states of TiO_2. The shift of the electronic charge inside the complex, and the resulting increase in reducing power of TiO_2/DA particles compared to bare TiO_2, is a consequence of an induced dipole moment upon surface modification.

Charge Separation. For the successful chemical reactivity of photogenerated charges, it is not enough to block surface trapping sites. To suppress their recombination reaction, it is also necessary to achieve large separation distances between photogenerated electrons and holes (free or trapped). Our approach to achieving enlarged separation distances is to remove one of the photogenerated charges such as photogenerated holes by strong coupling of electron-donating agents to the nanoparticle surface. For this purpose, we linked carboxyethyl-β-cyclodextrin, CE-β-CD, to TiO_2/DA particles. The linkage was obtained by condensation of a carboxyl group of cyclodextrin with an amino group of dopamine into a peptide bond. For comparison, bare TiO_2 particles were modified also with CE-β-CD linked to surface Ti atoms through carboxyl groups of cyclodextrin. β-Cyclodextrin with its seven sugar molecules was chosen as a multiple charge relay for possible tailored semiconductor-receptor design.[52] Due to the relative hydrophobicity of their inner cage, cyclodextrins are generally used as host molecules in host−guest inclusion complexes of water-insoluble compounds. The ability of electrons to reduce silver nitrate on the surface of particles is used as a probe of the efficient extended charge separation of photogenerated carriers.[53]

The production of metallic silver upon photogeneration of electrons and holes in semiconductor particles was monitored visually as a darkening of dry spots for the samples containing the following nanocrystallites: (1) bare TiO_2, (2) TiO_2/CE-β-CD, (3) TiO_2/DA, and (4) TiO_2/DA/CE-β-CD. The 10 mM molar concentration of TiO_2 was used in all solutions. Surface Ti atoms of TiO_2/CE-β-CD particles were linked to carboxyl groups of CE-β-CD and contained 40 CE-β-CD molecules/particle, while surface Ti atoms of TiO_2/DA/CE-β-CD were linked to CE-β-CD via a dopamine bridge and have only 2 CE-β-CD molecules/particle. The experimental design was achieved by placing 6 μL of each solution on a glass slide. After drying in air, 6 μL of 10 mM solution of $AgNO_3$ was added on each spot and again dried in air. All spots on the slide were exposed simultaneously to the white light from a 300-W Xe lamp for 3 min. The slide was positioned perpendicular to the source of light in order to achieve optimal geometry for all four spots. Figure 7 presents a photographic image of the slide after illumination. The darkening of spots is directly related to the amount of deposited silver metal.[52] As can be seen from Figure 7, the most efficient reduction of silver was obtained for cyclodextrin linked to TiO_2 particles via a dopamine bridge, although only 2 CE-β-CD molecules/particle are present. When this is compared with CE-β-CD linked to TiO_2 through carboxyl groups, the difference is significant, especially if the ratio of cyclodextrins per particle is taken into account (2:1 for TiO_2/DA/CE-β-CD and 40:1 for TiO_2/CE-β-CD). The results suggest that dopamine can be used as a relay for linking electron-donating molecules for efficient charge separation. The increased reducing power of TiO_2/DA particles by some 100 mV compared to bare TiO_2 makes reduction of silver more favorable. The slight difference between photoactivity of bare and dopamine-modified TiO_2 is a result of the higher reducing power of delocalized electrons and/or larger absorption of visible light of TiO_2/DA (due to the red shift of the absorption edge of dopamine-modified particles[13]).

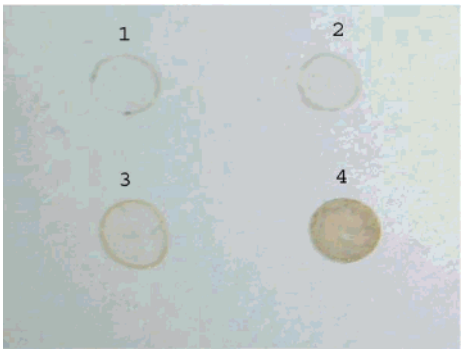

Figure 7. Photographic image of dry samples after photoexcitation with white light from a 300-W Xe lamp. The dry samples contain 60 nmol of $AgNO_3$ and (1) bare TiO_2, (2) carboxyethyl-β-cyclodextrin-linked TiO_2 (40:1), [TiO_2/CE-β-CD], (3) dopamine-modified TiO_2 [TiO_2/DA], and (4) carboxyethyl-β-cyclodextrin-linked dopamine-modified TiO_2 particles (2:1) [TiO_2/DA/CE-β-CD]. The concentration of titanium, 0.1 μmol, was the same in all four samples.

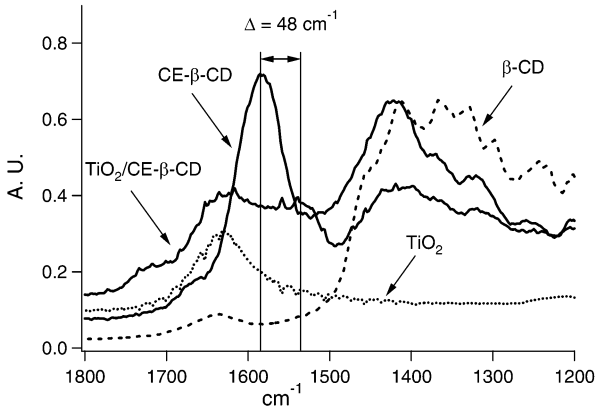

Figure 8. FTIR spectra of carboxyethyl-β-cyclodextrin (CE-β-CD), β-cyclodextrin (β-CD), carboxyethyl-β-cyclodextrin-linked TiO_2 (TiO_2/CE-β-CD), and bare TiO_2.

Our results also suggest that the bidentate dopamine complex is more efficient for charge separation than the carboxyl complex with surface Ti atoms. This is of particular importance as most of the dyes couple to the surface Ti atoms via carboxyl groups.[1b,53] In that respect, carboxyethyl-β-cyclodextrin behaves as any other molecule with carboxyl groups, forming a chelating complex with Ti atoms at the surface of TiO_2. This was confirmed by Fourier transform infrared (FTIR) spectroscopy. Figure 8 presents the change of vibration spectrum of CE-β-CD after linkage to TiO_2. Figure 8 also contains spectra of bare TiO_2 and β-cyclodextrin, β-CD. The band at 1583 cm^{-1} of CE-

β-CD, which is absent in β-CD, corresponds to the carbon−oxygen double bond stretching vibration, ν(C═O), of the symmetrical carboxyl group. Upon adsorption of CE-β-CD onto TiO_2 particles, the band shifts toward higher energies and is assigned to carbon−oxygen single bond stretching frequency, ν(C−O) of the metal−ligand complex.[54] The small difference, $\Delta = 48\ cm^{-1}$, between two frequencies is characteristic of the bidentate complex.[55]

In conclusion, optical absorption spectra of excess injected electrons in dopamine-capped TiO_2 nanoparticles display monotonic featureless energy dependence (investigated for $0.6 \leq E \leq 2.0$ eV), in contrast to the bare particle, which exhibits two preferential optical transitions with energies in the visible region of the light spectrum ($E_{max} = 1.9$ and 1.4 eV) corresponding to deep electron trapping sites. These results indicate that, upon removal of coordinately unsaturated Ti sites at the TiO_2 nanoparticle surface, the excess injected electrons are either weakly localized on the shallow lattice sites or delocalized in the conduction band of nanoparticles. Capping of TiO_2 nanoparticles with dopamine was found to enhance the reducing power of electrons by 100 mV. The strong coupling of dopamine modifier was found to improve the efficiency of separation of photogenerated charges as manifested by enhanced deposition of metallic silver.

Acknowledgment. TEM analysis was carried out in the Electron Microscopy Collaborative Research Center at Argonne National Laboratory. This work was supported by the U.S. Department of Energy, Office of Basic Energy Sciences, Division of Chemical Sciences, under Contract W-31-109-Eng-38.

References and Notes

(1) For comprehensive reviews see (a) Hoffman, M. R.; Martin, S. T.; Choi, W.; Bahnemann, D. W. *Chem. Rev.* **1995**, *95*, 69; (b) Hagfeldt, A.; Gratzel, M. *Chem. Rev.* **1995**, *95*, 49; (c) Mills, A.; LeHunte, S. *J. Photochem. Photobiol. A: Chem.* **1997**, *108*, 1, and references therein.

(2) Fox, M. A. *Top. Curr. Chem.* **1987**, *142*, 71.

(3) Gerischer, H.; Heller, A. *J. Phys. Chem.* **1991**, *95*, 5261.

(4) Ollis, D. F., Al-Ekabi, H., Eds. Photocatalytic Purification and Treatment of Water and Air; Proceedings of the 1st International Conference on TiO_2 Photocatalytic Purification and Treatment of Water and Air, London, Ontario, Canada, 8−13 November 1992; *Trace Met. Environ.* **1993**, *3*.

(5) O'Regan, B.; Graetzel, M. *Nature* (*London*) **1991**, *353*, 737.

(6) Nasr, C.; Liu, D.; Hotchandani, S.; Kamat, P. V. *J. Phys. Chem.* **1996**, *100*, 11054.

(7) Meyer, G. J. *J. Chem. Educ.* **1997**, *74*, 652.

(8) Ellingson, R. J.; Asbury, J. B.; Ferrere, S.; Ghosh, H. N.; Sprague, J. R.; Lian, T.; Nozik, A. J. *Z. Phys. Chem.* (*Muenchen*) **1999**, *212*, 77.

(9) Huber, R.; Sporlein, S.; Moser, J. E.; Gratzel, M.; Wachtvetl, J. *J. Phys. Chem. B.* **2000**, *104*, 8995.

(10) Rajh, T.; Nedeljkovic, J. M.; Chen, L. X.; Poluektov, O.; Thurnauer, M. C. *J. Phys. Chem. B* **1999**, *103*, 3515.

(11) Thurnauer, M. C.; Rajh, T.; Tiede, D. M. *Acta Chem. Scand.* **1997**, *51*, 610.

(12) Chen, L. X.; Liu, T.; Thurnauer, M. C.; Csencsits, R.; Rajh, T. *J. Phys. Chem. B* **2002**, *106*, 8539.

(13) Rajh, T.; Chen, L. X.; Lukas, K.; Liu, T.; Thurnauer, M. C.; Tiede, D. M. *J. Phys. Chem. B* **2002**, *106*, 10543.

(14) Chen, L. X.; Rajh, T.; Wang, Z.; Thurnauer, M. C. *J. Phys. Chem. B* **1997**, *101*, 10688.

(15) Rajh, T.; Ostafin, A. E.; Micic, O. I.; Tiede, D. M.; Thurnauer, M. C. *J. Phys. Chem.* **1996**, *100*, 4538.

(16) (a) Banwarth, W.; Schmidt, D.; Stallard, R. L.; Hornung, C.; Knorr, R.; Muller, F. *Helv. Chim. Acta* **1988**, *71*, 2085. (b) Bonacheva, M.; Schibler, L.; Lincon, P.; Vogel, H.; Akerman, B. *Langmuir* **1999**, *15*, 4317.

(17) Dimitrijevic, N. M.; Bartels, D. M.; Jonah, C. D.; Takahashi, K.; Rajh, T. *J. Phys. Chem. B* **2001**, *105*, 954.

(18) Schuler, R. H.; Patterson, L. K. *J. Phys. Chem*. **1980**, *84*, 2088.

(19) Buxton, G. V.; Stuart, C. R. *J. Chem. Soc., Faraday Trans*. **1995**, *91*, 279.

(20) Howe, R. F.; Graetzel, M. *J. Phys. Chem*. **1985**, *89*, 4495.

(21) Serpone, N.; Lawless, D.; Khairutdinov, R.; Pelizzetti, E. *J. Phys. Chem*. **1995**, *99*, 16655.

(22) Nozik, A. J.; Memming, R. *J. Phys. Chem*. **1996**, *100*, 13061.

(23) Colombo, D. P.; Bowman, R. M. *J. Phys. Chem*. **1996**, *100*, 18445.

(24) Schlichthorl, G.; Huang, S. Y.; Sprague, J.; Frank, A. J. *J. Phys. Chem. B* **1997**, *101*, 8141.

(25) Boschloo, G.; Fitzmaurice, D. *J. Phys. Chem. B* **1999**, *103*, 2228.

(26) Dunghong, D.; Ramsden, J.; Gratzel, M. *J. Am. Chem. Soc*. **1982**, *104*, 2977.

(27) Henglein, A. *Ber. Bunsen-Ges. Phys. Chem*. **1982**, *86*, 241.

(28) Dimitrijevic, N. M.; Savic, D.; Micic, O. I.; Nozik, A. J. *J. Phys. Chem*. **1984**, *88*, 4278.

(29) Safrany, A.; Gao, R.; Rabani, J. *J. Phys. Chem. B* **2000**, *104*, 5848.

(30) Hart, E. J.; Anbar, M. *The Hydrated Electron*; Wiley: New York, 1970.

(31) Stanbury, D. M. *Adv. Inorg. Chem*. **1989**, *33*, 69.

(32) Ward, M. D.; White, J. R.; Bard, A. J. *J. Am. Chem. Soc*. **1983**, *105*, 27.

(33) Nozik, A. J. *Annu. Rev. Phys. Chem*. **1978**, *29*, 189.

(34) Gao, R.; Safrany, A.; Rabani, J. *Radiat. Phys. Chem.* **2002**, *65*, 599.

(35) Maity, D. K.; Mohan, H.; Mittal, J. P. *J. Chem. Soc., Perkin Trans. 2* **1994**, 919.

(36) Pankove, J. I. *Optical Processes in Semiconductors*. Prentice-Hall: Englewood Cliffs, NJ, 1971; p 75.

(37) Turner, G. M.; Beard, M. C.; Schmuttenmaer, C. A. *J. Phys. Chem. B* **2002**, *106*, 11716.

(38) Wu, Z. Y.; Ouvrard, G.; Gressier, P.; Natoli, C. R. *Phys. Rev. B* **1997**, *55*, 10382.

(39) Szczepankiewicz, S. H.; Moss, J. A.; Hoffman, M. R. *J. Phys. Chem. B* **2002**, *106*, 2922.

(40) Cline, J. A.; Jonah, C. D.; Bartels, D. M. *Rev. Sci. Instrum*. **2002**, *73*, 3908.

(41) Rajh, T.; Saponjic, Z. V.; Micic, O. I. *Langmuir* **1992**, *8*, 1265.

(42) Breitenkamp, M.; Henglein, A.; Lilie, J. *Ber. Bunsen-Ges. Phys. Chem*. **1976**, *80*, 973.

(43) Graetzel, M.; Frank, A. J. *J. Phys. Chem*. **1982**, *86*, 2964.

(44) Brown, G. T.; Darwent, J. R.; Fletcher, D. I. *J. Am. Chem. Soc*. **1985**, *107*, 6446.

(45) Mulvaney, P.; Swayambunathan, V.; Grieser, F.; Meisel, D. *Langmuir* **1990**, *6*, 555.

(46) Zang, L.; Rodgers, M. A. J. *J. Phys. Chem. B* **2000**, *104*, 468.

(47) Yan, S. G.; Prieskorn, Y. K.; Hupp, J. T. *J. Phys. Chem. B* **2000**, *104*, 10871.

(48) Neta, P.; Huie, R.; Ross, A. B. *J. Phys. Chem. Ref. Data* **1988**, *17*, 1027.

(49) Farrington, J. A.; Ebert, M.; Land, E. J. *J. Chem. Soc., Faraday Trans. 1* **1978**, *74*, 665.

(50) Meisel, D.; Mulac, W. A.; Matheson, M. S. *J. Phys. Chem*. **1981**, *85*, 179.

(51) Watanabe, T.; Honda, K. *J. Phys. Chem*. **1982**, *86*, 2617.

(52) Willner, I.; Eichen, Y. *J. Am. Chem. Soc.* **1987**, *109*, 6862.

(53) Rajh, T.; Nedeljkovic, J. M.; Chen, L. X.; Tiede, D. M.; Thurnauer, M. C. *J. Adv. Oxid. Technol*. **1998**, *3*, 292.

(54) Nakamoto, K. *Infrared and Raman Spectra of Inorganic and Coordination Compounds. Part B*: *Applications in Coordination, Organometallic and Bioinorganic Chemistry*; John Wiley & Sons: New York, 1997; pp 57−62.

(55) Deacon, G. B.; Phillips, R. J. *Coord. Chem. Rev*. **1980**, *33*, 227.